Morphology control by modulated synthesis of metal-organic framework CPO-27

Mali H. Rosnes,[a] Fredrik S. Nesse,[a] Martin Opitz,[a,†] and Pascal D. C. Dietzel[a,*]

[a]Department of Chemistry, University of Bergen, P.O. Box 7803, N-5020 Bergen, Norway.

†Current address: Forschungsinstitut Edelmetalle + Metallchemie, Katharinenstraße 17, 73525 Schwäbisch Gmünd, Germany.

*Email: Pascal.Dietzel@uib.no

KEYWORDS: CPO-27-M, MOF-74, Metal-Organic Framework, Crystal Shape, Morphology, ESI-MS, Crystal Engineering, Modulator approach.

ABSTRACT: The CPO-27/MOF-74 series is among the most investigated metal-organic frameworks because of their usefulness in a diverse range of applications. For specific applications, it will be important to control the shape and size of the crystallites of the material. The modulation approach has been successfully used to direct these parameters in the synthesis of MOFs. Here, we report the synthesis of CPO-27-Ni in the presence of different ratios of benzoic acid and acetic acid as modulators. Yields, powder X-ray diffraction data, scanning electron microscopy results, and elemental, thermogravimetric, and gas sorption analyses are compared to study the influence of the modulator on the product. The results show that we have successfully synthesized pure CPO-27-Ni independent of the amount of modulator. The modulator affects the resulting morphology of the crystalline product with a defined variation of particle sizes and shapes. In addition, ESI-MS has been employed in probing the reaction solutions. It shows the preferred formation of complexes between the metal cation and the modulator, thus indicating that the ligand substitution plays a major role in the crystal growth.

1. Introduction Metal-organic frameworks (MOFs) or porous coordination polymers (PCPs) are materials of infinite coordination networks composed of metal centers linked by organic ligands in a manner that leads to pores within the framework. They are often associated with high specific surface areas and are promising for use in a variety of applications [1-5]. The CPO-27-M series (see Fig. 1), also denoted M_2(dhtp), M_2(dobdc) (dhtp / dobdc = $C_8H_2O_6^{4-}$) or M-MOF-74, where M = Co [6], Ni [7], Mg [8], Mn [9], Zn [10], Fe [11-12], Cu [1,13-14], and Cd [15], along with mixed metal analogues [16], belong to the class of permanently porous MOFs with open metal sites. The metal centers in the structure are all coordinated to a solvent molecule, which can be removed upon heating and vacuum, leaving the metal centers with a non-occupied coordination site (open metal sites) available for interaction with adsorptives [1,6-7,17-22]. Among the originally reported solvothermal synthetic procedures for the preparation of CPO-27-Ni, there is actually a large variation in the solvent systems that were employed. Pure product was obtained in either tetrahydrofurane (THF) and water [7,23], or *N*,*N*'-dimethylformamide (DMF) [24]. Recently, CPO-27-Ni has been prepared in a "greener" procedure using only water as the solvent [25-28].

For many applications, it is important to be able to control the shape, size and uniformity of the crystallites or particles of the material to ensure homogeneity of the properties in the industrial process. As an example, one will frequently prefer smaller particles of homogeneous shape and size to minimize diffusion limitations in porous materials [29], or specific shapes of anisotropic crystals to achieve correct orientation in membranes [30-31]. Precise control over the crystallization process is a crucial contribution for achieving uniform particle sizes and shapes and homogeneity of properties. In 2009, Kitagawa *et al.* reported that it is possible to influence the equilibrium governing the self-assembly process in a MOF synthesis by adding a capping reagent

(a modulator) with the same chemical functionality as the organic linker inherent to the particular synthesis. The modulator interferes with the formation of coordinative bonds between the metal ions and linker, and its presence generates a competitive situation that regulates the rate of framework extension and crystal growth [32]. Additionally, the modulator may affect the synthesis through influencing the pH level [33-34]. The use of modulating agents in MOF syntheses has proven to be an excellent strategy for controlling the size and/or morphology of MOF crystals [33-41].

Herein, we focus on how benzoic acid influences the product of the synthesis reaction of CPO-27-Ni. Some acetic acid results are included for comparison. Both modulators have the same carboxylic acid functional group as the organic linker (H_4dhtp), see right hand side of Fig. 1, inherent to the production of CPO-27. To the best of our knowledge, there are only two reports where monocarboxylic acids are investigated as modulators in the synthesis of CPO-27 (MOF-74) [42-43]. Pachfule *et al.* utilised salicylic acid as a modulator in the fabrication of rod-shaped MOF-74 [43]. It was found that the addition of salicylic acid modulator directed MOF growth in a rod-shaped morphology by stabilizing the active metal sites on the MOF crystal surface. More recently, Albuquerque *et al.* used benzoic acid in microwave-assisted synthesis to improve the uniformity of the Ni-MOF-74 product [42]. It was found that the modulator (benzoic acid) and the H_4dhtp linker competitively react with Ni^{2+} during the synthesis, which can decrease the reagent conversion and also modify the crystal morphology. Herein, we present the first comprehensive investigation into the effects benzoic acid and acetic acid have on the resulting CPO-27 materials synthesized under solvothermal conditions.

Electrospray ionization mass spectrometry (ESI-MS) has been employed previously in studying the formation of materials such as zeolites and MOFs [44-51]. Here, we use the technique to probe

the reaction solutions and investigate the influence of benzoic acid on the synthesis of CPO-27-Ni and -Co.

2. Experimental section

2.1 Instrumentation

Scanning electron microscopy (SEM). A ZEISS Supra 55VP scanning electron microscope was used. Filament: field emission. kV range: 100 V to 30 kV. STEM detector, EDX detector for element analyses, WDS detector for element analyses, backscatter detector, cathode luminescence detector and variable pressure detector. The samples were prepared for SEM analysis by sputter coating with gold under vacuum.

Elemental analysis (EA). CHN analyses were carried out on an Elementar vario EL III.

Thermogravimetric analysis-differential scanning calorimeter (TG-DSC). A Netzsch Jupiter STA 449 F1 was used for simultaneous TG-DSC measurements. The temperature program ran from 30 to 600 °C, with a heating rate of 2 °C min^{-1} and a gas flow of 50 mL min^{-1} using an 80/20 mixture of Ar/O_2.

Powder X-ray diffraction (PXRD). Diffraction data was collected in Bragg-Brentano geometry using flat disc-shaped sample holders using a Bruker AXS D8 Advance, equipped with a 9 position multisampler, and monochromatic Cu $K_{\alpha 1}$ radiation. Whole powder pattern fitting of the PXRD data using the Pawley method were performed using TOPAS 4.2 to establish phase purity and obtain the crystallite size using full width at half maximum and integral breadth approach [52]. No reference material was used to obtain an instrumental resolution function to calibrate the numerical values of the crystallite sizes. For the purpose of this study, comparison of the crystallite sizes of different samples relative to each other is sufficient. Peak shapes were

refined using the functions provided by the TOPAS software to account for crystallite size effects using a Lorentzian and Gaussian convolution. The software calculates the crystallite size corresponding to the full width at half maximum and integral breadth approach from these parameters.

Gas adsorption. Nitrogen adsorption measurements were carried out on a BELSORP-max instrument at -196 °C to confirm the specific surface area and pore volume for the different samples. The samples were prepared under inert conditions and transferred to the sample cell in a glove box. Prior to the measurements, the samples were treated at 150 °C for 24 hours in a dynamic vacuum.

ESI-MS. Data was recorded using an Agilent 6420A triple quadrupole (QqQ configuration) mass analyser using electrospray ionisation (ESI). It was connected to an Agilent 1200 series LC module (binary pump, column compartment/oven and auto sampler). The eluent stream was introduced directly into the source, at a dry gas temperature of 200 °C. The ion polarity for all MS scans recorded was positive, with the voltage of the capillary tip set at 3500 V. Fragmentor at 175 V and cell accelerator voltage of 7 V.

ESI-MS was used to investigate the effect of the modulator (benzoic acid) on the synthesis of CPO-27-Ni using a mixture of 1 mmol $M(OAc)_2{\cdot}4H_2O$, 0.5 mmol H_4dhtp and 0.5 mmol benzoic acid in a water-THF solvent system. Additional measurements for the analogous synthesis of CPO-27-Co were performed to help with the assignment of chemical species to *m*/*z* traces. In a typical experiment, an aliquot was taken from the supernatant solution of the reaction mixture after a pre-defined period time and diluted 1/10 to avoid overloading the detector. Initial reaction solution were sampled within 2 minutes after combination. The reaction solutions were then heated to 110

°C and followed by ESI-MS over time, from 30 min to overnight. All experiments have been reproduced several times with the same results.

Materials. All chemicals, reagents and solvents were purchased from Sigma-Aldrich and used as received without further purification. CPO-27–Ni was synthesized under solvothermal conditions. The samples used for gas adsorption measurements were processed under inert conditions. Gases used for gas adsorption measurements were of 99.9995%, or higher, purity and were purchased from Yara Praxair.

2.2 Synthesis

Preparation of $[Ni_1(C_4H_1O_3)(H_2O)_1]\cdot 4H_2O$ (CPO-27–Ni) in pure water without modulator. A mixture of 2,5-dihydroxyterephthalic acid (0.099 g, 0.5 mmol) and nickel(II) acetate tetrahydrate (0.249 g, 1.0 mmol) were dissolved in H_2O (12 mL) in a Teflon-lined insert (23 mL volume). After stirring for 5-10 min the insert was placed in an autoclave, sealed and reacted for up to 24 h at 110 °C in a preheated furnace. The yellow crystalline product was obtained by filtration, and washed with H_2O and ethanol (EtOH), before being left to dry in air. The yields for ($[Ni_1(C_4H_1O_3)(H_2O)_1]\cdot 4H_2O$) are listed in Table S2. A list of the average EA results is shown in Table S1. Powder X-ray diffraction confirmed the identity of the compound. The samples prepared for gas sorption measurements were filtered and dried under inert conditions.

Preparation of $[Ni_1(C_4H_1O_3)(H_2O)_1]\cdot 4H_2O$ (CPO-27–Ni) in water and EtOH (or THF) with modulator. 2,5-dihydroxyterephthalic acid (0.099 g, 0.5 mmol) was dissolved in EtOH or THF (6 mL), before modulator (benzoic or acetic acid) (0-30 mmol) was added, and the mixture was stirred for 5 min. Nickel(II) acetate tetrahydrate (0.249 g, 1.0 mmol) was dissolved in H_2O (6 mL). The two mixtures were combined and stirred for another 5-10 min in a Teflon-lined insert (23 mL volume) before the insert was placed in an autoclave, sealed and reacted for up to 24 h at 110 °C

in a preheated furnace. Whereas the amount of H_4dhtp and $Ni(OAc)_2 \cdot 4H_2O$ were kept constant, the amount of modulator was varied between 0 and 30 mmol. The yellow crystalline products of CPO-27-Ni were obtained by filtration, and washed with H_2O and EtOH, before being left to dry in air. The yields are listed in Table S2. A list of the average EA results for each modulator amount is listed in Table S1. Powder X-ray diffraction confirmed the identity of the compounds. The work up for the samples used in the gas sorption measurements differed in that the product was filtered and dried under inert conditions.

For further information of experimental details, see section 1 in the SI.

3. Results and Discussion

To investigate the influence of benzoic acid and acetic acid as modulators in the preparation of CPO-27-Ni we set out to synthesize the material with constant amounts of nickel(II) acetate and H_4dhtp, whilst varying the amount of modulator from 0 to 30 mmol. To allow for such large amounts of benzoic acid the modulated syntheses were carried out in a 1:1 mixture by volume of H_2O and EtOH (and in some cases THF). For comparison reasons we also carried out the reactions in absence of modulator in the same 1:1 (*v:v*) H_2O:EtOH/THF mixtures. To ensure reproducibility and reliability each of the benzoic acid reactions in H_2O and EtOH were carried out three times, and yield, PXRD and SEM were recorded for each of these. In addition, we performed experiments using acetic acid in H_2O and THF.

We compare the products obtained using varying amounts of modulator with a sample obtained using a variation of the method reported by Guasch *et al.*[27] (see experimental section). The highly crystalline samples of CPO-27-Ni obtained without use of a modulator had a BET specific surface area of 1340 $m^2\ g^{-1}$.

3.1 PXRD analysis. All the samples were characterized by powder X-ray diffraction. Figure 2 shows the normalized results for the three non-modulated reactions, 0.5 and 1 mmol benzoic acid in H_2O and THF, and for 0.5-30 mmol benzoic acid in H_2O and EtOH. The PXRD pattern for a material synthesized in H_2O and THF with 15 mmol acetic acid is shown in Figure S3, confirming that these reaction conditions result in formation of CPO-27-Ni.

The crystallite size of the various products was obtained from Pawley profile fits. No reference material was used to obtain an instrumental resolution function to calibrate the numerical values, which means the absolute values have limited meaning. However, they do allow comparison of the crystallite size in the different samples relative to each other, i.e. whether the crystallites in one sample are larger or smaller than in another. For the non-modulated syntheses, the solvent system has a clear effect on the crystallite size (Table S3). For either solvent mixture (H_2O and THF or H_2O and EtOH) there are reductions in the observed crystallite sizes compared to pure H_2O. There is a much smaller difference in crystallite size for the different reaction conditions in the presence of the modulator. As the amount of modulator is increased, there is only a slight increase in crystallite size. Thus, the data indicate that the modulator does affect the crystallite size only to a minor degree, and a much larger effect is actually due to the solvent system used in the reaction.

3.2 Elemental analysis, thermogravimetric analysis and yield. Elemental analyses (Table S1) and thermogravimetric analyses (Figure S1) were carried out to compare the products of the different syntheses, ensuring that the results, independent of the method used, resulted in the same composition. This confirms that we have successfully synthesized the hydrated CPO-27-Ni material with either solvent combination or modulator. The EA and TG data do not indicate the presence of significant amounts of modulator in the pores.

While there is no significant difference in yield for the different solvent systems in absence of a modulator, there are clear effects on the yield for the different solvent combinations depending on type and amount of modulator (see Table S2). The yields when using benzoic acid as the modulator, in either H_2O/EtOH and H_2O/THF, follow similar trends, and the solvent combination appears to have a smaller influence than the choice of modulator. For most amounts of benzoic acid as modulator, the yields are lower than in the non-modulated reactions for both solvent combinations. There is a general trend of decreasing yields as the amount of benzoic acid is increased. One might argue that the product formation might be slowed down by competitive complexation of the metal ion with the modulating agent. Longer reaction times might then lead to increased yields. We performed a few exploratory syntheses with longer reaction time of 7d for selected modulator concentrations in H_2O/EtOH, for which we did not observe any significant change in yield, which indicates that the precipitation reaction had reached equilibrium conditions already after 1d. In addition, we observe that the yields vary a lot when the amount of the modulator is high (especially for 20 and 30 mmol benzoic acid in the water-EtOH solvent system), which indicates that the yield is heavily dependent of the mixing of the reactants. The large amount of modulator makes it more difficult to stir and mix the reactants perfectly reproducible in the individual reactions. Such a decreasing trend in yields as for benzoic acid as modulator is not apparent for acetic acid. In fact, acetic acid in H_2O and THF results in the highest yields for any given amount of modulator, in some cases even higher than for the non-modulated syntheses.

3.3 Scanning electron microscopy (SEM). The morphology of the products from each of the experiment was investigated using SEM. As discussed in section 3.1, the crystallite size as calculated from PXRD patterns appears to vary only little as an effect of the presence of the modulator in the syntheses. In contrast, the SEM micrographs of the different samples do show a

significant change in size and morphology of the CPO-27-Ni particles. Particles are frequently composed of multiple crystallites, and in those cases one would expect them to be larger. Particle size and shape vary significantly as a direct consequence of the amount of modulator used in the synthesis, as can be seen exemplarily in Figure 3 for syntheses with 0 to 30 mmol benzoic acid. Micrographs of samples when using both benzoic acid and acetic acid in H_2O and THF are shown in sections 7.3 and 7.4, respectively, in the SI.

The choice of solvent system has a direct effect on the morphology and size of the CPO-27-Ni product already in the absence of a modulator, which is clearly visible in Figure 3a (synthesis in H_2O) and 3b (synthesis in H_2O and EtOH). When only water is used in the synthesis as sole solvent, the product consists of well-defined hexagonal needle shaped crystals of up to 10 μm in length, even though there is significant heterogeneity in size (Figure 3a, see also section 7.1.1 in SI). Clearly, the crystals grew predominantly along the [001] direction, resulting in larger crystals with more anisotropic and better-defined shape. In contrast, when the synthesis was performed in a 50:50 *v:v* mixture of water and EtOH, the product consists of significantly smaller circular agglomerates of around 5 μm in diameter (Figure 3b, section 7.1.3). Similar features are observed when using water and THF as solvent system (section 7.1.2 in the SI), for which the product consists of smaller spherical agglomerates of crystallites.

Upon addition of the modulator within a given solvent system, we observe a change in product morphology in dependence of the concentration of modulator. Size and shape of the product deviate from the product obtained without use of a modulating agent. Using 0.5 mmol of benzoic acid in ethanol and water (Figure 3c) we see similar agglomerates as for 0 mmol in water and ethanol (Figure 3b), but the agglomerates appear to be growing closer together and are even connected. In both cases, they consist of smaller crystals originating from the centers of the

spheres. When 1 mmol of benzoic acid is employed, the agglomerates are less spherical and more like large compact units (Figure 3d). The individual crystallites appear to be larger than for the three previous reaction conditions. For 2.5 mmol of benzoic acid, the morphology changes more dramatically (Figure 3e). The product appears to consist of larger particles of about 10 μm diameter, which actually consist of smaller inter-grown crystals agglomerated into larger "pillar" like crystals. With 5 mmol of benzoic acid, we obtain product with a mixture of morphologies (Figure 3f). It contains some smaller hexagonal needle-shaped crystals and much larger compact block-like particles. These larger crystals become more needle shaped for synthesis with 10 and even more pronounced with 15 mmol benzoic acid (Figures 3g and h, respectively). For 20 mmol of benzoic acid, the product is dominated by needle-shaped crystals, which range from very thin crystallites to larger, thicker and longer needles (Figure 3i). The morphology of the product changes again with addition of 30 mmol of benzoic acid, for which we observe a uniform product of thin, needle-shaped crystals that resembles the product obtained in the synthesis using only water as solvent (Figure 3j).

The results when using a mixture of water and THF as the solvent system (shown in section S7.3 in the SI) are very similar to the results in the water-EtOH system for the low amounts of modulator, but as the amount of modulator is increased, there is a significant difference observed between the two solvent systems. While the water-EtOH system result in better-defined needle shaped crystals when using large amounts of modulator, the water-THF system leads to larger block crystals.

We have also investigated how the morphology of the product changes when acetic acid is used as modulator instead of benzoic acid in the water and THF solvent system (see section 7.4 in the SI). Whilst using benzoic acid typically results in homogenous and reproducible samples, the

products when using acetic acid were more varied, despite our best efforts to perform the syntheses exactly alike. Using 5 mmol acetic acid results in fascinating compact inter-gown particles displaying what looks like orthogonal angles. With larger amounts of acetic acid, we typically observe two morphologies of the product, one of which consists of small, compact hexagonal needle-shaped crystals and the other consists of larger compact crystals. However, using 30 mmol acetic acid in water and THF sometimes produce perfectly shaped needle crystals, similar to the pure water synthesis, such as have been observed previously by Pachfule *et al.* when utilising salicylic acid as a modulator in the fabrication of rod-shaped MOF-74 [43]. Clearly, the nature of the modulating agent can have a significant effect on the product morphology.

3.4 Gas sorption measurements. Gas sorption measurements were carried out to investigate whether there is an effect of the modulator on the textural properties of the product. The gas sorption properties are one of the main reasons why MOF materials such as CPO-27-Ni are so interesting [1-3]. It is known that the adsorption properties of the compounds in the CPO-27 series are negatively affected by handling the material under ambient conditions after synthesis [23,53-55]. We therefore repeated a selection of the experiments, where the samples were filtrated and subsequently handled under inert conditions. The solvent was exchanged with methanol by immersion for 30 minutes and subsequent filtration; this process was repeated three times. The materials were then dried under vacuum at 150 °C for 24 h before the sorption experiments were carried out. The resulting textural properties are listed in Table 1, with the corresponding isotherms available in section 8 in the SI. The measurement were focused on syntheses with benzoic acid as modulator in H_2O and EtOH, but one experiment using H_2O and THF, as well as one acetic acid in H_2O and THF are included for comparison.

It is apparent that in the absence of modulator, there is no significant effect of the solvent system on the textural properties (see three first entries in Table 1), which have values indicating full accessibility to the pores [23]. Introduction of 1 and 5 mmol benzoic acid to the synthesis leads to a minor reduction in specific surface area and pore volume (<5 %), independent of the solvent mixture. As the amounts of modulator are increased further, there is a gradual reduction in specific surface area and pore volume. The lowest specific surface area is observed for 30 mmol benzoic acid in H_2O and EtOH, where it is only around 74 % of what is obtained for the non-modulated reactions. In general, the textural properties of the modulated syntheses vary more than what we observe for the non-modulated syntheses. This might be because there is still a very small amount of modulator remaining in the product and possibly blocking access to some channels. The amounts necessary to have such an effect are well below what one would expect to be observable in the elemental analysis. An attempt to remove such potentially remaining modulator molecules by extending the solvent exchange with methanol to 24 h did not show a significant change in the textural properties.

3.5 ESI-MS analyses. ESI-MS was performed to investigate the effect of benzoic acid as modulator on the synthesis of CPO-27-Ni. While a modulator is typically introduced in large excess in the syntheses of MOFs [18,32], we could use only lower concentrations of benzoic acid in the ESI-MS studies due to the sensitivity of the instrument. Thus, a reaction mixture of 1 mmol $M(OAc)_2{\cdot}4H_2O$, 0.5 mmol H_4dhtp and 0.5 mmol benzoic acid in a water-THF solvent system was used. Any effects such a small amount of modulator has in solution will only be acerbated at the more typical higher concentrations.

The assignments for ESI-MS spectra (Figure 4) the species present in the initial mixture of both nickel(II) and cobalt(II) acetate tetrahydrate, respectively, with 2,5-dihydroxyterepthalic acid and

benzoic acid are listed in Table 2. The most dominating species at *m/z* 77.0 and 105.0 have both been assigned to benzoic acid, whilst *m/z* 134.9/135.9 have been assigned to the nickel/cobalt acetate starting materials, respectively. The remaining species labelled in Figure 4 have been assigned to metal species coordinated to acetate and/or benzoic acid. These species are also observed for mixtures of $M(OAc)_2 \cdot 4H_2O$ and benzoic acid that were prepared without adding 2,5-dihydroxyterephthalic acid. In our experience, non-coordinated H_4dhtp is difficult to ionize into the gas phase and observe by ESI-MS in positive mode, explaining its absence from the spectra.

When the reaction mixtures are heated at 110 °C, there are very few changes in the spectra over a time period of up to 24 h, even compared to the initial mixture at room temperature, except that the overall intensities are reduced, species at higher *m/z* become even less intense, and the resulting spectra look busier compared to the initial ones. Based on the fact that we see little to no evidence of species that can be assigned to H_4dhtp coordinated to Ni^{2+}/Co^{2+} it is evident that benzoic acid competes with H_4dhtp for the coordination sites on Ni^{2+}/Co^{2+}. Species of the metal cation coordinated to the modulator dominate the spectrum, rather than those of the metal cation coordinated with the organic linker molecule. The coordination network of the MOF can only be built up if the modulator ligand is replaced by a linking ligand, and it feels safe to assume that it is this additional ligand substitution that steers the crystallization under the different modulator concentrations explored in this paper to yield the variation in morphologies we have observed.

It has been argued whether the effect the presence of the excessive amounts of modulator has on the pH of the synthesis reaction is the dominating factor in determining the crystallization product [32-34]. Our observation that even addition of low ratios of modulator lead to predominant formation of adducts between the metal cation and modulator indicate that the ligand substitution plays a major role in the crystal growth.

4. Conclusions. We have studied the effect of using benzoic acid and acetic acid as modulators on the synthesis of CPO-27-Ni. Syntheses were carried out using a range of modulator amounts to elucidate systematic effects on the resulting morphology of the product. Irrespective of the nature or amount of modulator or solvent mixture used, we successfully synthesized phase pure CPO-27-Ni but differed in yield and morphology.

We find that the morphology of the CPO-27-Ni products is influenced by all three factors: (i) the solvent system; (ii) the amount of modulator; and (iii) the chemical nature of the modulator. In water as solvent and in the absence of a modulator, well-defined needle-shaped crystals are observed, whilst smaller agglomerates are obtained in water-EtOH and water-THF solvent systems. Upon addition of low concentrations of benzoic acid as modulator, we observe little difference in morphology for the samples obtained in the water-EtOH and water-THF systems. When using higher concentrations of benzoic acid, better-defined needle shaped crystals are obtained in the water-EtOH system, while larger block crystals are formed in the water-THF system. The use of acetic acid as modulator typically lead to two different morphologies of the product, one of which consists of hexagonal needle-shaped crystals and the other consists of larger compact crystals.

The specific surface area and pore volume of CPO-27-Ni samples prepared in the different solvent systems without use of a modulator were the same and indicated full access to the pores. The addition of a modulator did lead to a decrease in the specific surface area and pore volume that scaled with the amount of modulator. Even with the highest concentrations of modulator, high surface area materials were still obtained.

Analysis of the reaction mixtures during the synthesis of CPO-27-Ni and -Co by ESI-MS revealed how even small amounts of benzoic acid significantly influence the species present in the

reaction solution. This confirms that there is a competition for the coordination of the metal cation between the organic linker and the modulator. The ESI-MS data indicate that there is a preference for the benzoic acid to coordinate the metal cation when the reactants are still in the solution. The additional ligand substitution required to build the coordination network in the presence of a modulator is likely to lead to the increase in particles size, just as observed.

In summary, the modulator approach has been shown to be useful in obtaining CPO-27 with a defined variation of particle sizes and shapes.

Acknowledgments

The authors would like to thank Dr. Bjarte Holmelid for ESI-MS advice, and the Laboratory for Electron Microscopy at the Faculty of Mathematics and Natural Sciences at UiB. The authors would also like to acknowledge the support from the Research Council of Norway through the FRINATEK program (grant 221596) and ISP-KJEMI program (grant 209339).

REFERENCES

(1) M. H. Rosnes, M. Opitz, M. Frontzek, W. Lohstroh, J. P. Embs, P. A. Georgiev, P. D. C. Dietzel, J. Mater. Chem. A 3 (2015) 4827-4839.
(2) P. D. C. Dietzel, V. Besikiotis, R. Blom, J. Mater. Chem. 19 (2009) 7362-7370.
(3) P. Valvekens, M. Vandichel, M. Waroquier, V. Van Speybroeck, D. De Vos, J. Catal. 317 (2014) 1-10.
(4) H. F. Yao, Y. Yang, H. Liu, F. G. Xi, E. Q. Gao, J. Mol. Catal. A-Chem. 394 (2014) 57-65.
(5) P. K. Allan, P. S. Wheatley, D. Aldous, M. I. Mohideen, C. Tang, J. A. Hriljac, I. L. Megson, K. W. Chapman, G. De Weireld, S. Vaesen, R. E. Morris, Dalton Trans. 41 (2012) 4060-4066.
(6) P. D. C. Dietzel, Y. Morita, R. Blom, H. Fjellvåg, Angew. Chem. Int. Ed. 44 (2005) 6354-6358.
(7) P. D. C. Dietzel, B. Panella, M. Hirscher, R. Blom, H. Fjellvåg, Chem. Commun. (2006) 959-961.
(8) P. D. C. Dietzel, R. Blom, H. Fjellvåg, Eur. J. Inorg. Chem. 2008 (2008) 3624-3632.
(9) W. Zhou, H. Wu, T. Yildirim, J. Am. Chem. Soc. 130 (2008) 15268-15269.
(10) N. L. Rosi, J. Kim, M. Eddaoudi, B. Chen, M. O'Keeffe, O. M. Yaghi, J. Am. Chem. Soc. 127 (2005) 1504-1518.

(11) E. D. Bloch, L. J. Murray, W. L. Queen, S. Chavan, S. N. Maximoff, J. P. Bigi, R. Krishna, V. K. Peterson, F. Grandjean, G. J. Long, B. Smit, S. Bordiga, C. M. Brown, J. R. Long, J. Am. Chem. Soc. 133 (2011) 14814-14822.
(12) M. Märcz, R. E. Johnsen, P. D. C. Dietzel, H. Fjellvåg, Micropor. Mesopor. Mat. 157 (2012) 62-74.
(13) G. Calleja, R. Sanz, G. Orcajo, D. Briones, P. Leo, F. Martínez, Catal. Today 227 (2014) 130-137.
(14) R. Sanz, F. Martínez, G. Orcajo, L. Wojtas, D. Briones, Dalton Trans. 42 (2013) 2392-2398.
(15) M. Díaz-García, M. Sánchez-Sánchez, Micropor. Mesopor. Mat. 190 (2014) 248-254.
(16) L. J. Wang, H. Deng, H. Furukawa, F. Gándara, K. E. Cordova, D. Peri, O. M. Yaghi, Inorg. Chem. 53 (2014) 5881-5883.
(17) P. D. C. Dietzel, R. E. Johnsen, R. Blom, H. Fjellvåg, Chem. Eur. J. 14 (2008) 2389-2397.
(18) A. Schaate, P. Roy, A. Godt, J. Lippke, F. Waltz, M. Wiebcke, P. Behrens, Chem. Eur. J. 17 (2011) 6643-6651.
(19) J. L. C. Rowsell, O. M. Yaghi, J. Am. Chem. Soc. 128 (2006) 1304-1315.
(20) M. Dincă, W. S. Han, Y. Liu, A. Dailly, C. M. Brown, J. R. Long, Angew. Chem. Int. Ed. 46 (2007) 1419-1422.
(21) Y.-G. Lee, H. R. Moon, Y. E. Cheon, M. P. Suh, Angew. Chem. Int. Ed. 47 (2008) 7741-7745.
(22) J. G. Vitillo, L. Regli, S. Chavan, G. Ricchiardi, G. Spoto, P. D. C. Dietzel, S. Bordiga, A. Zecchina, J. Am. Chem. Soc. 130 (2008) 8386-8396.
(23) P. D. C. Dietzel, P. A. Georgiev, J. Eckert, R. Blom, T. Strassle, T. Unruh, Chem. Commun. 46 (2010) 4962-4964.
(24) S. R. Caskey, A. G. Wong-Foy, A. J. Matzger, J. Am. Chem. Soc. 130 (2008) 10870-10871.
(25) S. Cadot, L. Veyre, D. Luneau, D. Farrusseng, E. Alessandra Quadrelli, J. Mater. Chem. A 2 (2014) 17757-17763.
(26) L. Garzon-Tovar, A. Carne-Sanchez, C. Carbonell, I. Imaz, D. Maspoch, J. Mater. Chem. A 3 (2015) 20819-20826.
(27) J. Guasch, P. D. C. Dietzel, P. Collier, N. Acerbi, Micropor. Mesopor. Mat. 203 (2015) 238-244.
(28) D. Cattaneo, S. J. Warrender, M. J. Duncan, R. Castledine, N. Parkinson, I. Haley, R. E. Morris, Dalton Trans. 45 (2016) 618-629.
(29) D. Schneider, D. Mehlhorn, P. Zeigermann, J. Kärger, R. Valiullin, Chem. Soc. Rev. 45 (2016) 3439-3467.
(30) S. Japip, Y. Xiao, T.-S. Chung, Ind. Eng. Chem. Res. 55 (2016) 9507-9517.
(31) B. Seoane, J. Coronas, I. Gascon, M. E. Benavides, O. Karvan, J. Caro, F. Kapteijn, J. Gascon, Chem. Soc. Rev. 44 (2015) 2421-2454.
(32) T. Tsuruoka, S. Furukawa, Y. Takashima, K. Yoshida, S. Isoda, S. Kitagawa, Angew. Chem. Int. Ed. 48 (2009) 4739-4743.
(33) Z. G. Hu, I. Castano, S. N. Wang, Y. X. Wang, Y. W. Peng, Y. H. Qan, C. L. Chi, X. R. Wang, D. Zhao, Cryst. Growth Des. 16 (2016) 2295-2301.
(34) B. Seoane, S. Castellanos, A. Dikhtiarenko, F. Kapteijn, J. Gascon, Coord. Chem. Rev. 307 (2016) 147-187.

(35) R. J. Marshall, C. L. Hobday, C. F. Murphie, S. L. Griffin, C. A. Morrison, S. A. Moggach, R. S. Forgan, J. Mater. Chem. A 4 (2016) 6955-6963.
(36) S. Hermes, T. Witte, T. Hikov, D. Zacher, S. Bahnmüller, G. Langstein, K. Huber, R. A. Fischer, J. Am. Chem. Soc. 129 (2007) 5324-5325.
(37) S. Diring, S. Furukawa, Y. Takashima, T. Tsuruoka, S. Kitagawa, Chem. Mater. 22 (2010) 4531-4538.
(38) A. Umemura, S. Diring, S. Furukawa, H. Uehara, T. Tsuruoka, S. Kitagawa, J. Am. Chem. Soc. 133 (2011) 15506-15513.
(39) G. Zahn, P. Zerner, J. Lippke, F. L. Kempf, S. Lilienthal, C. A. Schroder, A. M. Schneider, P. Behrens, CrystEngComm 16 (2014) 9198-9207.
(40) E. A. Flugel, A. Ranft, F. Haase, B. V. Lotsch, J. Mater. Chem. 22 (2012) 10119-10133.
(41) W. Morris, S. Wang, D. Cho, E. Auyeung, P. Li, O. K. Farha, C. A. Mirkin, ACS Appl. Mater. Interfaces 9 (2017) 33413-33418.
(42) G. H. Albuquerque, G. S. Herman, Cryst. Growth Des. 17 (2017) 156-162.
(43) P. Pachfule, D. Shinde, M. Majumder, Q. Xu, Nature Chem. 8 (2016) 718-724.
(44) G. Seeber, G. J. T. Cooper, G. N. Newton, M. H. Rosnes, D.-L. Long, B. M. Kariuki, P. Kogerler, L. Cronin, Chem. Sci. 1 (2010) 62-67.
(45) J. A. Rood, W. C. Boggess, B. C. Noll, K. W. Henderson, J. Am. Chem. Soc. 129 (2007) 13675-13682.
(46) I. H. Lim, W. Schrader, F. Schüth, Chem. Mater. 27 (2015) 3088-3095.
(47) J. A. Rood. Metal-Organic Frameworks as Functional, Porous Materials. University of Notre Dame, Notre Dame, Indiana, 2009.
(48) I. H. Lim, W. Schrader, F. Schüth, Micropor. Mesopor. Mat. 166 (2013) 20-36.
(49) S. J. Garibay, Z. Wang, K. K. Tanabe, S. M. Cohen, Inorg. Chem. 48 (2009) 7341-7349.
(50) J. S. Mathieson, G. J. T. Cooper, A. L. Pickering, M. Keller, D.-L. Long, G. N. Newton, L. Cronin, Chem. Asian J. 4 (2009) 681-687.
(51) J. S. Mathieson, M. H. Rosnes, V. Sans, P. J. Kitson, L. Cronin, Beilstein J. Nanotechnol. 4 (2013) 285-291.
(52) A. A. Coelho, J. Evans, I. Evans, A. Kern, S. Parsons, Powder Diffr. 26 (2012) S22-S25.
(53) D. Yu, A. O. Yazaydin, J. R. Lane, P. D. C. Dietzel, R. Q. Snurr, Chem. Sci. 4 (2013) 3544-3556.
(54) J. Liu, A. I. Benin, A. M. B. Furtado, P. Jakubczak, R. R. Willis, M. D. LeVan, Langmuir 27 (2011) 11451-11456.
(55) A. C. Kizzie, A. G. Wong-Foy, A. J. Matzger, Langmuir 27 (2011) 6368-6373.

Table and Figure Captions

Table 1. Results from gas sorption analysis, N_2 at -196 °C.

Table 2. Assignment of the most dominant species in the spectra of initial 1:0.5:0.5 mmolar ratio mixtures of $M(OAc)_2 \cdot 4H_2O$:H_4dhtp and benzoic acid. M = Co and Ni.

Figure 1. (a) The desolvated framework structure of CPO-27-Ni, molecular structure of (b) the organic linker H_4dhtp and the modulators (c) benzoic acid and (d) acetic acid.

Figure 2. Comparison of normalized PXRD patterns obtained using the different reaction conditions (BA = benzoic acid).

Figure 3. CPO-27-Ni synthesized in (a) pure water without modulator and (b-j) water and EtOH, with addition of (b) 0 mmol; (c) 0.5 mmol; (d) 1 mmol; (e) 2.5 mmol; (f) 5 mmol; (g) 10 mmol; (h) 15 mmol; (i) 20; and (j) 30 mmol benzoic acid. More information is available in section 7.2 in the SI.

Figure 4. Representative ESI-MS results of the initial mixture of 1:0.5:0.5 mmolar ratio $Co(OAc)_2 \cdot 4H_2O$, H_4dhtp and benzoic acid (blue) and 1:0.5:0.5 mmolar ratio $Ni(OAc)_2 \cdot 4H_2O$, H_4dhtp and benzoic acid (green).

Table 1. Results from gas sorption analysis, N_2 at -196 °C.

Modulator amount / mmol	**Modulator** (acid)	**Solvent system**	**BET** / $m^2\ g^{-1}$	**Pore volume** / $cm^3\ g^{-1}$ (calculated at p/p_0=0.5)	**Langmuir** / $m^2\ g^{-1}$
0	none	H_2O	1342	0.52	1475
0	none	H_2O/THF	1331	0.53	1513
0	none	H_2O/EtOH	1356	0.52	1486
1.0	Benzoic	H_2O/EtOH	1304	0.50	1439
5.0	Benzoic	H_2O/EtOH	1295	0.49	1404
5.0	Benzoic	H_2O/THF	1315	0.49	1390
10.0	Benzoic	H_2O/EtOH	1181	0.46	1316
15.0	Benzoic	H_2O/EtOH	1029	0.40	1136
15.0	Acetic	H_2O/THF	1173	0.46	1309
20.0	Benzoic	H_2O/EtOH	1039	0.40	1144
30.0	Benzoic	H_2O/EtOH	990	0.38	1073

Table 2. Assignment of the most dominant species in the spectra of initial 1:0.5:0.5 mmolar ratio mixtures of $M(OAc)_2{\cdot}4H_2O$:H_4dhtp and benzoic acid. M = Co and Ni.

m/z (Ni)	**Assigned to**	**m/z (Co)**
77.1	$[C_6H_5]^{1+}$	77.1
105.0	$[C_7H_5O]^{1+}$	105.0
134.9	$[M(CH_3COO)(H_2O)]^{1+}$	135.9
160.9	$[(C_7H_6O_2)K]^{1+}$	160.9
178.9	$[M(C_7H_5O_2)]^{1+}$	179.9
250.9	$[M_2(CH_3COO)_2(OH)]^{1+}$	252.9
300.9	$[M(C_7H_5O_2)(C_7H_6O_2)]^{1+}$	301.9
354.9	$[M_2(CH_3COO)_2(C_7H_5O_2)]^{1+}$	356.9
416.9	$[M_2(CH_3COO)(C_7H_5O_2)_2]^{1+}$	418.9
478.8	$[M_2(C_7H_5O_2)_3]^{1+}$	480.9

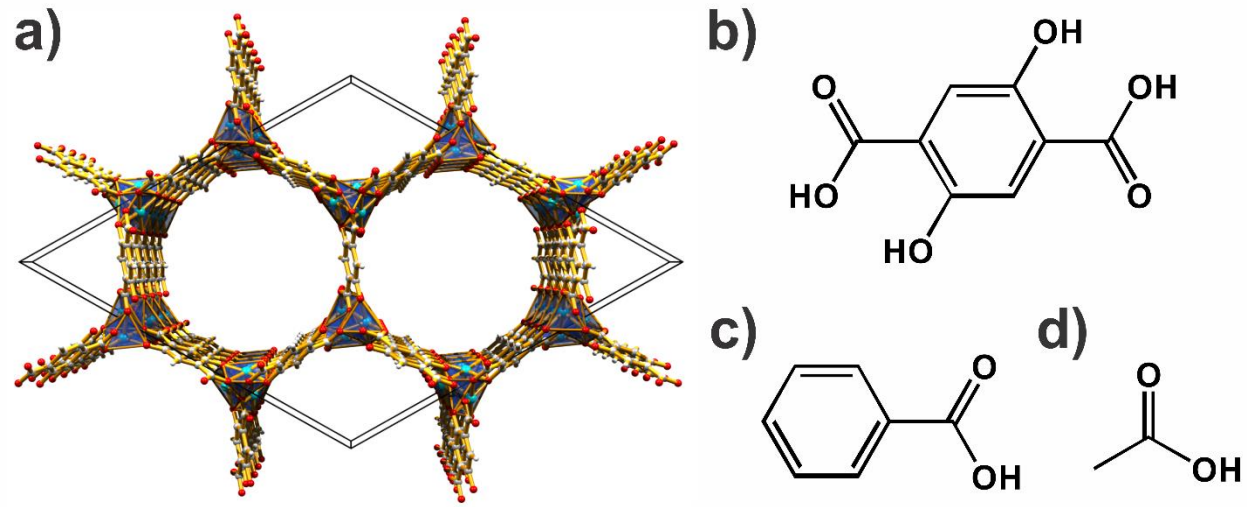

Figure 1. (a) The desolvated framework structure of CPO-27-Ni, molecular structure of (b) the organic linker H_4dhtp and the modulators (c) benzoic acid and (d) acetic acid.

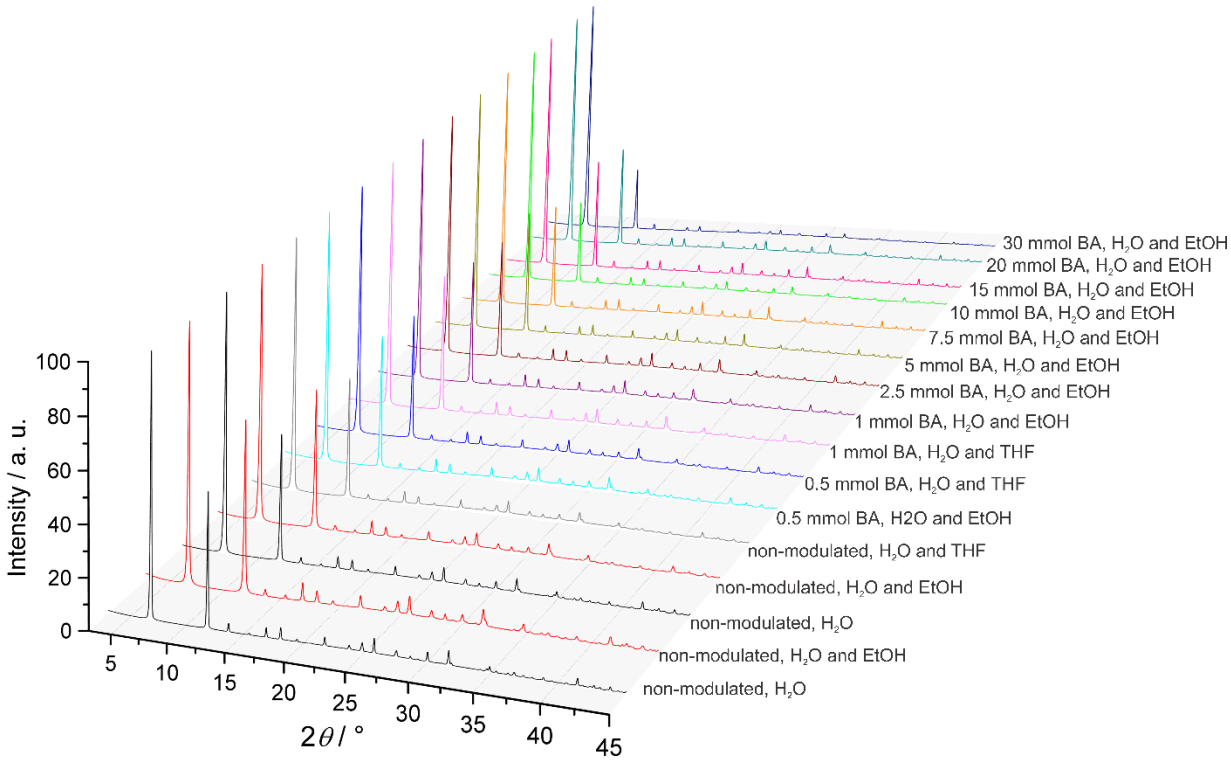

Figure 2. Comparison of normalized PXRD patterns obtained using the different reaction conditions (BA = benzoic acid).

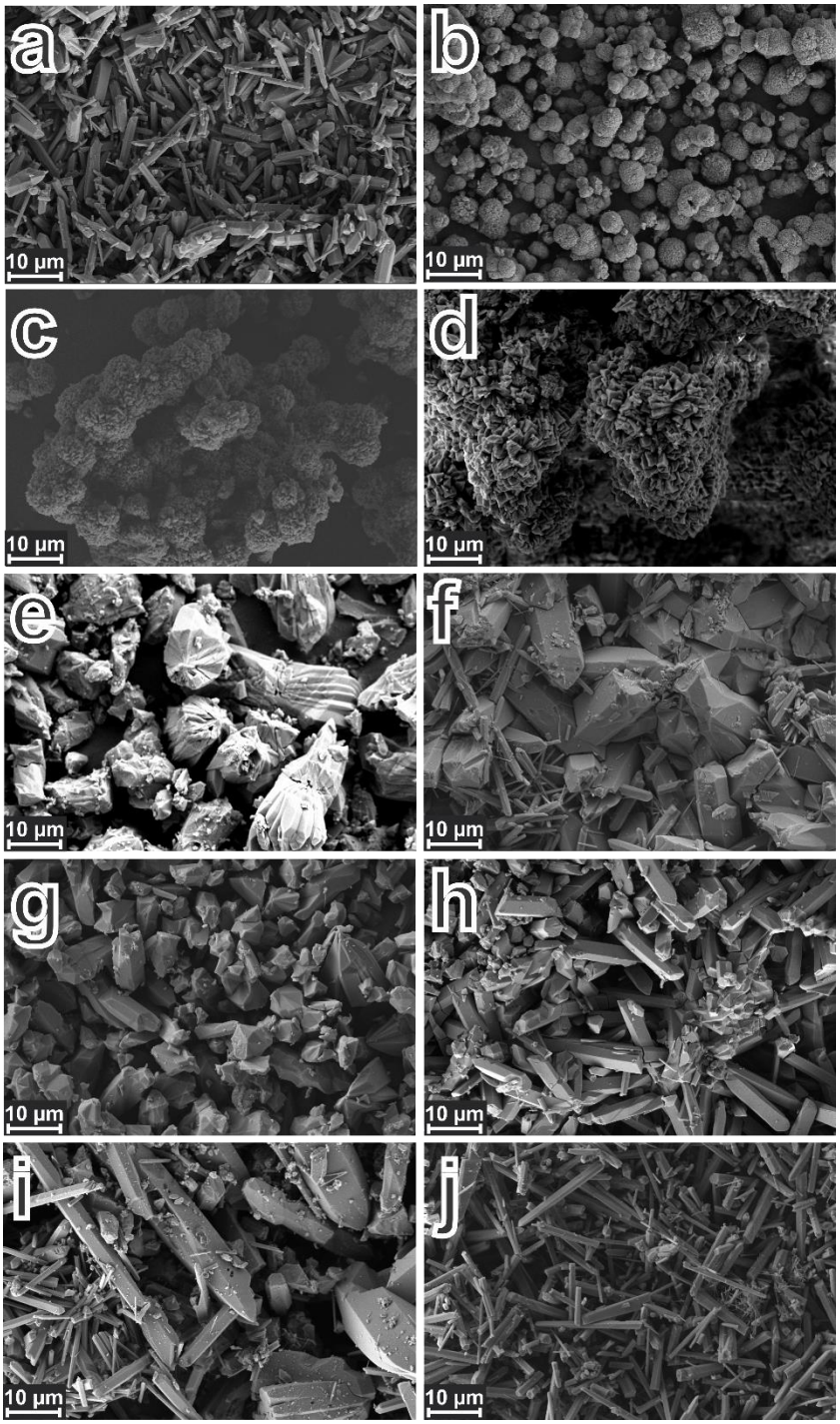

Figure 3. CPO-27-Ni synthesized in (a) pure water without modulator and (b-j) water and EtOH, with addition of (b) 0 mmol; (c) 0.5 mmol; (d) 1 mmol; (e) 2.5 mmol; (f) 5 mmol; (g) 10 mmol; (h) 15 mmol; (i) 20; and (j) 30 mmol benzoic acid. More information is available in section 7.2 in the SI.

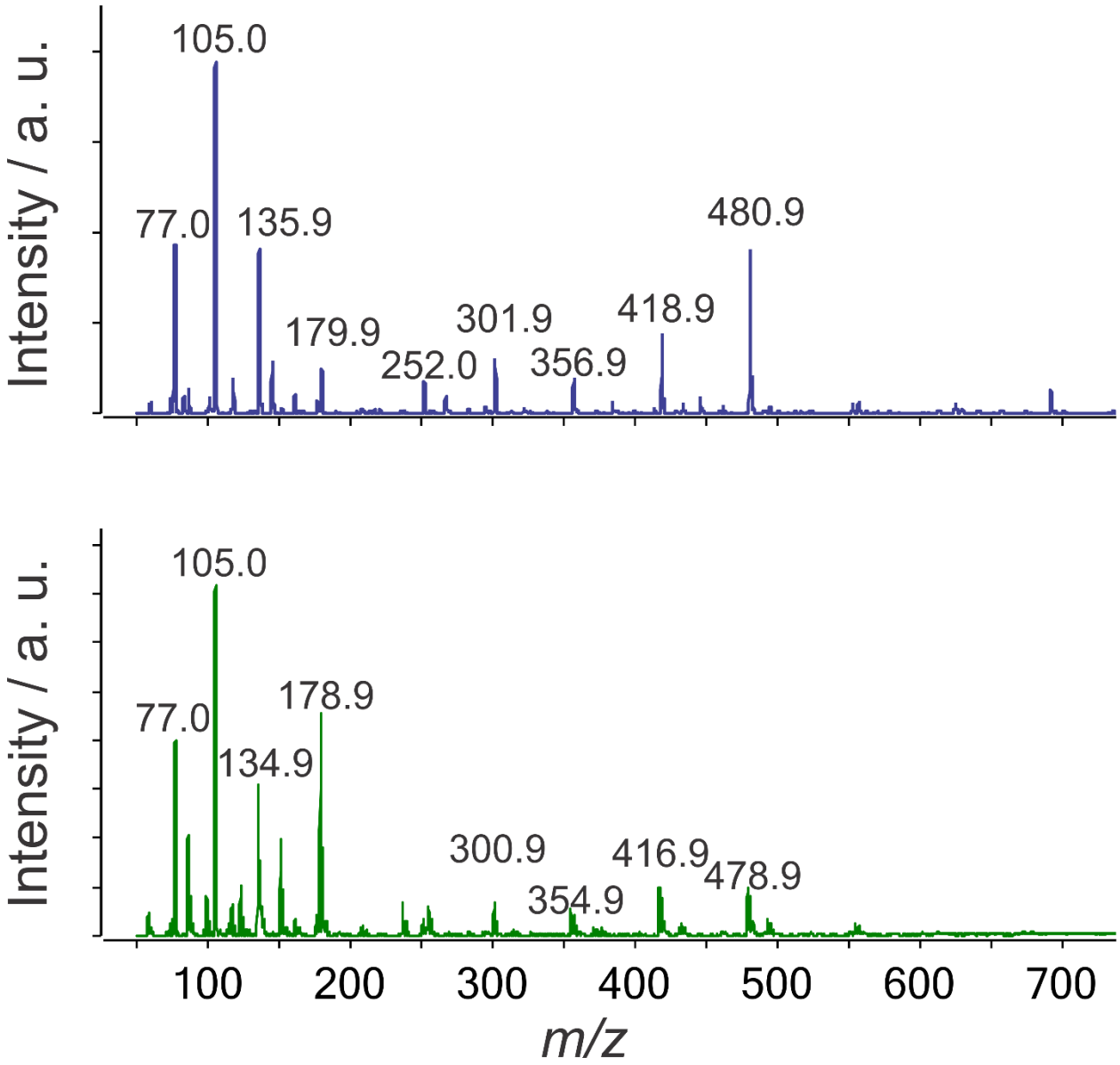

Figure 4. Representative ESI-MS results of the initial mixture of 1:0.5:0.5 mmolar ratio $Co(OAc)_2 \cdot 4H_2O$, H_4dhtp and benzoic acid (blue) and 1:0.5:0.5 mmolar ratio $Ni(OAc)_2 \cdot 4H_2O$, H_4dhtp and benzoic acid (green).